Invasion of Herpes Simplex Virus Type 1 into Murine Epidermis: An *Ex Vivo* Infection Study

Elena Rahn[1], Philipp Petermann[1], Katharina Thier[1], Wilhelm Bloch[2], Jessica Morgner[3], Sara A. Wickström[3,4] and Dagmar Knebel-Mörsdorf[1,5]

Herpes simplex virus type 1 (HSV-1) invades its human host via the skin or mucosa. We aim to understand how HSV-1 overcomes the barrier function of the host epithelia, and for this reason, we established an *ex vivo* infection assay initially with murine skin samples. Here, we report how tissue has to be prepared to be susceptible to HSV-1 infection. Most efficient infection of the epidermis was achieved by removing the dermis. HSV-1 initially invaded the basal epidermal layer, and from there, spreading to the suprabasal layers was observed. Strikingly, in resting stage hair follicles, only the hair germ was infected, whereas the quiescent bulge stem cells (SCs) were resistant to infection. However, during the growth phase, infected cells were also detected in the activated bulge SCs. We demonstrated that cell proliferation was not a precondition for HSV-1 invasion, but SC activation was required as shown by infection of aberrantly activated bulge SCs in integrin-linked kinase (ILK)-deficient hair follicles. These results suggest that the status of the bulge SCs determines whether HSV-1 can reach its receptors, whereas the receptors on basal keratinocytes are accessible irrespective of their proliferation status.

INTRODUCTION

Herpes simplex viruses types 1 and 2 (HSV-1, HSV-2) are ubiquitous pathogens that are well adapted to their human hosts. Upon primary infection via the skin and mucocutaneous regions, HSV can reach sensory neurons where latent infection is established. The extent of primary and recurrent mucocutaneous infections is largely a function of the host's immune status. HSV infections can be devastating in immune-compromised hosts and newborns. Normally, the skin forms an effective barrier to infection. However, patients with skin lesions are predisposed to primary, as well as recurrent HSV infections. Eczema herpeticum, a disseminated HSV-1 infection of the skin, is a complication of atopic dermatitis, suggesting the impaired epidermal barrier function and the dysregulated immune response as risk factors for higher susceptibility to HSV-1 (Wollenberg *et al.*, 2003; Bussmann *et al.*, 2008). In addition to atopic disease, skin abrasions or burns are particularly susceptible to HSV (Foley *et al.*, 1970; Shenoy *et al.*, 2015).

Although viral entry into individual cells in culture and the immune response to HSV have been studied in detail, we still have little knowledge of how the virus invades tissue and which cellular factors determine susceptibility to efficient HSV infection. Two important cellular factors are the surface receptors, herpes virus entry mediator (HVEM) and nectin-1, which interact with the viral envelope glycoprotein D (Montgomery *et al.*, 1996; Geraghty *et al.*, 1998). A further glycoprotein D receptor is 3-O-sulfated heparan sulfate (Shukla *et al.*, 1999; O'Donnell *et al.*, 2010). These receptors are essential for the fusion of the viral envelope with cellular membranes. In addition, heparan sulfate proteoglycans serve as attachment factors and thus bind the virus before it interacts with the cellular glycoprotein D receptors (Shieh *et al.*, 1992).

Mice are widely used as an animal model for studies of HSV skin, mucosal, and corneal infections, and the murine homologs of nectin-1 and HVEM support HSV-1 entry (Yoon *et al.*, 2003). Furthermore, infection studies with HSV-2 revealed that both nectin-1 and HVEM are needed for disease development in mice (Taylor *et al.*, 2007). Previously, we demonstrated that nectin-1, which is expressed on the surface of most epidermal keratinocytes, is important for HSV-1 entry into murine epidermis, whereas HVEM, which is restricted to a limited number of cells, can potentially replace nectin-1 as receptor (Petermann *et al.*, 2015). How HSV-1 invades the epidermis and reaches its receptors is still not known.

[1]Center for Biochemistry, University of Cologne, Cologne, Germany; [2]Department of Molecular and Cellular Sports Medicine, German Sports University, Cologne, Germany; [3]Paul Gerson Unna Group 'Skin Homeostasis and Ageing', Max Planck Institute for Biology of Ageing, Cologne, Germany; [4]Cologne Excellence Cluster on Cellular Stress Responses in Aging-Associated Diseases (CECAD), University of Cologne, Cologne, Germany and [5]Department of Dermatology, University of Cologne, Cologne, Germany

Correspondence: Dagmar Knebel-Mörsdorf, Center for Biochemistry and Department of Dermatology, University of Cologne, Joseph-Stelzmann-Strasse 52, Cologne 50931, Germany. E-mail: dagmar.moersdorf@uni-koeln.de

Scarification of the skin, mucosa, or cornea is generally used to infect mice efficiently, and, although this is clearly distinct from the natural invasion route, it has allowed various aspects of immune responses and viral pathogenesis to be studied. To analyze the initial infection steps in the epidermis, we established an *ex vivo* infection model using murine epidermal sheets as a tool to allow the analysis of cellular factors that determine HSV-1 susceptibility. In this paper, we characterize the *ex vivo* infection assay; we investigate how epidermal sheets have to be prepared to be susceptible to HSV-1, which cells can be infected, and whether cell proliferation contributes to viral entry. Our results indicate that basal as well as differentiated keratinocytes can be infected. The major precondition is cell viability, but infection does not require proliferation. Interestingly, quiescent stem cells (SCs) in the hair bulge were protected from HSV-1, whereas activation of SCs in the hair follicle growth phase or by genetical ablation of ILK led to infection of these cells as well.

RESULTS

Ex vivo infection of complete murine skin and epidermal sheets with HSV-1

We prepared murine tail skin to analyze susceptibility to HSV-1 by *ex vivo* infection. The skin samples were infected by submerging them in virus suspension, and infection was determined by staining the samples with an antibody against the viral protein ICP0 at various times post infection (p.i.). ICP0 is one of the first viral genes to be expressed once the viral genome is released into the nucleus (Boutell and Everett, 2013). At early times after infection, ICP0 localizes in nuclear foci, but it relocalizes to the cytoplasm later during infection (Petermann *et al.*, 2009). Thus, visualization of ICP0 expression indicates the successful entry of HSV-1 into individual cells. At 3 hours and even as late as 12 hours p.i., no ICP0 signals were detected in intact skin samples (Figure 1a), suggesting that HSV-1 cannot penetrate via either the cornified layer or the dermal layer. Also, at the edge of skin samples, no infected cells were detected. Even when the cornified layer was removed, nearly no infected cells were observed (data not shown). Only after removal of the dermis and infection of the epidermal sheets, was cytoplasmic ICP0 visible. It was present in the basal layer at 3 hours p.i. and spreading to suprabasal layers was observed as early as 6 hours p.i. (Figure 1b), demonstrating that nucleated keratinocytes can be infected. To confirm that all basal keratinocytes are susceptible to HSV-1, we visualized ICP0 in whole/mount preparations of epidermal sheets. The results indicated that all basal cells expressed cytoplasmic ICP0 at 3 hours p.i. when the epidermal sheets were infected at 100 plaque-forming unit (PFU)/cell. Infection at 10 PFU/cell resulted in fewer infected cells, and the predominantly nuclear location of ICP0 at 3 hours p.i. indicated a slower infection (Figure 1d).

Melanocytes represent the major class of non-keratinocyte cells in the epidermis (Lin and Fisher, 2007). In contrast to Langerhans cells (Sprecher and Becker, 1986), another class of non-keratinocytes in the epidermis, susceptibility of melanocytes to HSV-1 is still unknown. Our results demonstrate that the very few murine melanocytes, which were present in primary keratinocyte cultures (characterized by tyrosinase expression), were infected (Figure 1e). As nectin-1 serves as the major receptor for HSV-1 on keratinocytes (Petermann *et al.*, 2015), we also analyzed the behavior of melanocytes isolated from nectin-1-deficient epidermis. Surprisingly, melanocytes could be infected in the absence of nectin-1 (Figure 1e). These results demonstrate the susceptibility of melanocytes to HSV-1 even in the absence of nectin-1 implying the use of alternative receptor(s).

As the visualization of ICP0 expression detects only the onset of infection, we next determined production of progeny virus by plaque assays. As expected, viruses were produced upon infection of epidermal sheets (from 2×10^2 to 3×10^6 PFU/ml) (Figure 1c). In contrast, infection of intact skin with even a high virus dose (50 PFU/cell) led to a very small but a consistent increase in virus progeny (from 3×10^4 to 1×10^5 PFU/ml) (Figure 1c). These results suggest that at least some cells in the skin sample can be productively infected even though there was no detectable ICP0 expression (Figure 1a).

When isolated epidermal sheets were pre-incubated in medium for extended periods prior to infection, the number of infected cells in the basal layer decreased. In freshly prepared epidermal sheets or those pre-incubated for 3 hours, all basal keratinocytes were infected by 3 hours p.i. (Figure 2a and b). However, after pre-incubation for 16 hours, ICP0 expression could only be detected in 60% of cells, and very few infected cells were detected after 24 hours of pre-incubation (Figure 2a and b). The decreased number of infected cells correlated with an enlargement and flattening of basal keratinocytes (Figure 2a). In addition, when tight junctions (TJs) were visualized by ZO-1 staining, there was extensive relocalization throughout the epidermis following 16 hours of pre-incubation and 3 hours of infection (Figure 2c) indicative of TJ formation in the basal layer.

We further analyzed the transition of the basal keratinocytes in the incubated epidermal sheets by electron microscopy. After cultivation for 16 hours in medium, the transition into extremely flat cells in the basal layer became obvious (Figure 3a). Overall, the morphology of the epidermal sheets suggests a loss of cell polarity. In contrast, when epidermal sheets were analyzed directly after separation from the dermis, the basal layer showed no disturbance of morphology and architecture (Figure 3b). In the incubated sheets, the flat basal keratinocytes lost most of the keratin fibers, whereas suprabasal cells maintained at least some (Figure 3a). The intercellular spaces differed clearly between incubated and directly analyzed sheets. Although the wide intercellular spaces in non-incubated sheets were characterized by many contacting cell extensions and intact desmosomes, cell–cell contacts in the incubated sheets were much closer (Figure 3d and e, arrowheads). There was evidence for TJ formation in the basal layer (Figure 3d, arrowhead), which supports the ZO-1 staining of the incubated sheets (Figure 2c). In addition, incubation led to cell death in the basal as well as in the suprabasal layers, which was very rarely observed in non-incubated sheets. The decreased number of viable cells after incubation for 16 hours was confirmed by flow cytometric analysis (data not shown). Taken together, these
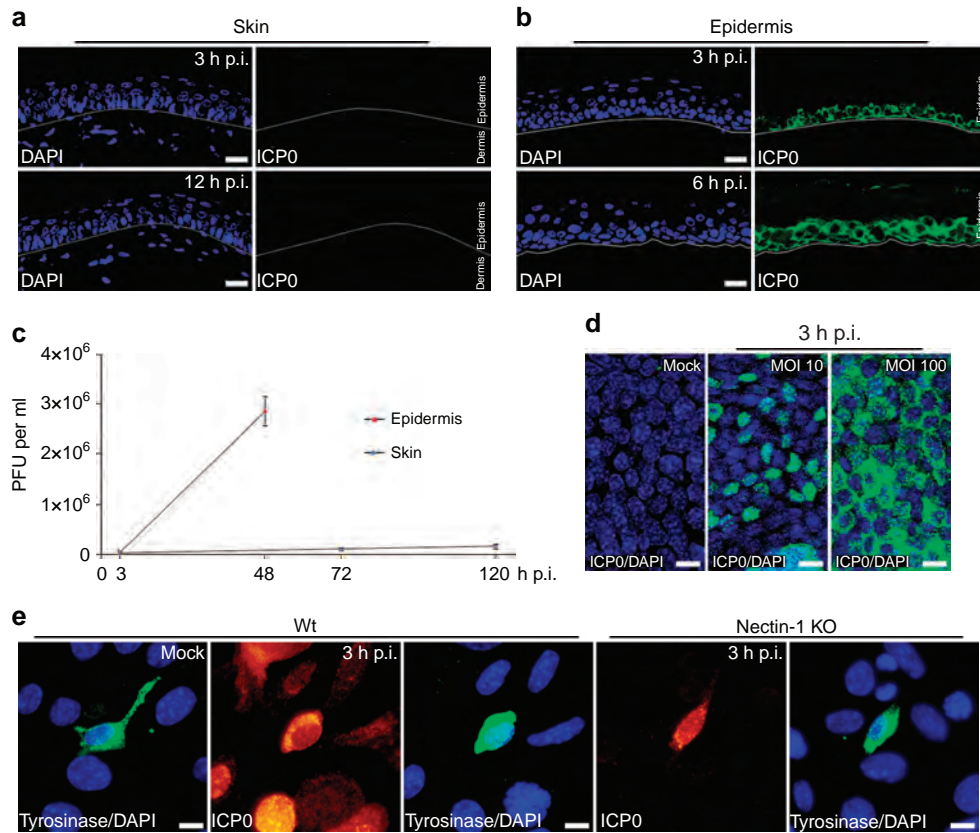
Figure 1. HSV-1 infects epidermal sheets and melanocytes but not skin samples. (**a**) Skin or (**b**) epidermal sheets from tails of 3-week-old mice were infected at 100 PFU/cell. White line = basement membrane. Immunostainings of the epidermis visualize ICP0 in the basal layer and viral spreading to suprabasal layers (**b**). (**c**) The virus titer was determined after infection of epidermises or the skin (n = 3). The epidermal sheets were infected at 1 PFU/cell, whereas the skin was infected at 50 PFU/cell to increase the chances of infection. (**d**) Infected whole mounts show infection in the basal layer. (**e**) Primary epidermal cells from wt or nectin-1-deficient mice were infected at 20 PFU/cell. Staining for tyrosinase visualizes melanocytes. Bars, 25 μm (**a** and **b**), 10 μm (**d**), and 4.5 μm (**e**). PFU, plaque-forming unit; wt, wild type.
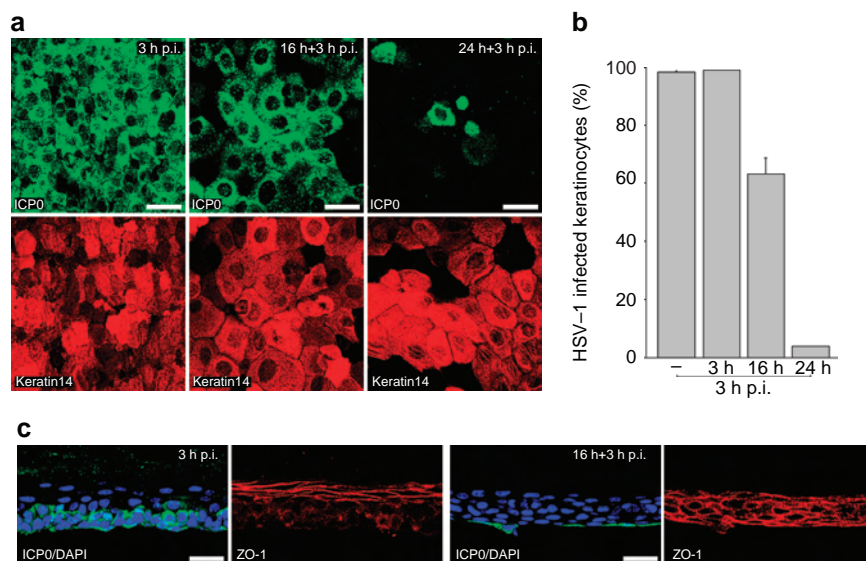

Figure 2. Pre-incubation of epidermal sheets influences susceptibility to HSV-1. (**a**) Epidermal sheets were infected at 100 PFU/cell directly after separation from the dermis by dispase II or after incubation in medium for 16 or 24 hours. Epidermal whole mounts were stained at 3 hours p.i. (**b**) Quantification of infected cells in epidermal sheets without incubation and in those that were incubated for 3, 16, and 24 hours. (**c**) Epidermal sheets that were either not incubated or incubated for 16 hours were infected at 100 PFU/cell. Immunostainings of ZO-1 in sections visualize TJs. Bars, 25 μm. PFU, plaque-forming unit; p.i., post infection; TJ, tight junction.
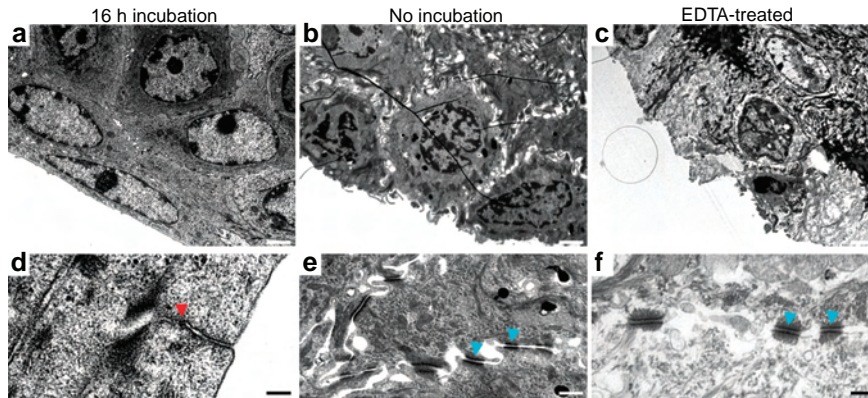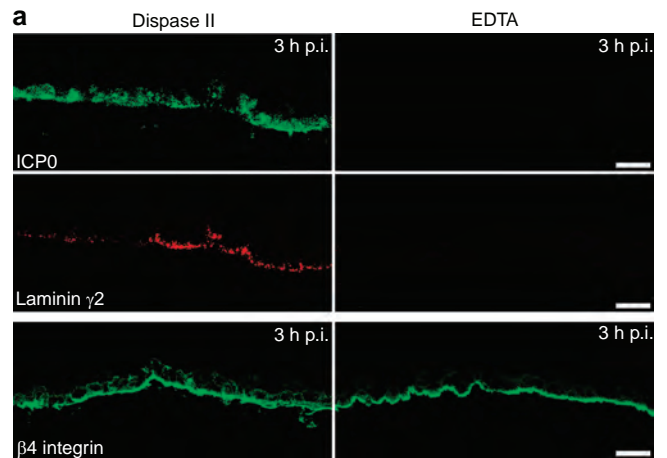
Figure 3. Cell morphology changes after incubation of epidermal sheets or after separation from the dermis by EDTA treatment. (**a**) Epidermal sheets separated by dispase II and either incubated for 16 hours in medium or (**b**) directly analyzed after separation, and (**c**) epidermises separated by EDTA treatment were analyzed by EM. (**a**, **b** and **c**) In addition to the basal layers, magnifications show TJ-like structures in the incubated sample (**d**) (indicated by red arrowhead), intact desmosomes connected to keratin filaments in the not incubated sample (**e**) (indicated by blue arrowheads), and desmosome complexes that were not connected to keratin filaments in the EDTA-treated sample (**f**). Bars, 2 μm (**a**, **b** and **c**), 0.12 μm (**d**), 0.5 μm (**e**), 0.3 μm (**f**). EM, electron microscopy; TJ, tight junction.

results suggest that the incubation of epidermal sheets for more than 16 hours in DMEM leads to an atypical differentiation process with a remodeling of TJs and decreased cell viability, which interferes with HSV-1 susceptibility.

In summary, we do not observe infected cells in skin samples upon *ex vivo* infection with HSV-1. However, as soon as the dermis is removed, HSV-1 can gain access to the epidermis via the basal layer provided that the epidermal sheets are only kept in culture for a limited time prior to infection and can then spread to suprabasal layers.

Ex vivo infection of epidermal sheets separated with either dispase II or EDTA

The above *ex vivo* infection studies with HSV-1 were performed in epidermal sheets that were separated from the dermis by dispase II treatment. Dispase II cleaves fibronectin and collagen IV, which disrupts attachment of the basement membrane while maintaining a viable and intact epidermal sheet (Gipson and Grill, 1982). We confirmed the loss of the basement membrane and the disruption of hemidesmosomes by electron microscopy (Figure 3b). Furthermore, we observed cellular extensions at the basal layer (Figure 3b), which have been described as preferred attachment sites for HSV-1 (Petermann *et al.*, 2015). To better preserve the hair follicles during the separation step, we applied the widely used EDTA treatment, which should facilitate the analysis of infected cells in the hair follicles (Braun *et al.*, 2003). Interestingly, no infected cells were observed in epidermal sheets separated with EDTA (Figure 4a). To exclude the possibility that components of the basement membrane were still present on EDTA-treated epidermal sheets, which might prevent virus attachment, we stained sections with various basement membrane markers. Although β4 integrin, a receptor for laminins, was detected on both dispase II and EDTA-treated sheets, integral components of the basement membrane such as the laminin γ2 chain, nidogen 1, and perlecan were only observed after dispase II treatment (Figure 4b). Collagen IV was not detected on either dispase II-

b

	Dispase II	EDTA
Laminin γ2	+	−
Collagen IV	−	−
β4 integrin	+	+
Nidogen 1	+	−
Perlecan	+	−

Figure 4. Lack of HSV-1 infection and the absence of basement membrane markers after EDTA treatment of epidermal sheets. (**a**) Epidermal sheets were separated from the dermis either by dispase II or by EDTA treatment and infected at 100 PFU/cell. Sections were stained at 3 hours p.i. Bars, 40 μm. (**b**) Summary of the presence/absence of markers in dispase II- or EDTA-treated epidermal sheets. HSV-1, Herpes simplex virus type 1; PFU, plaque-forming unit; p.i., post infection.

or on EDTA-treated samples (Figure 4b). This indicates that EDTA treatment dissociates the basement membrane more efficiently than dispase II. However, further analysis of EDTA-treated epidermal sheets by electron microscopy revealed that most of the basal keratinocytes were disrupted, characterized by nuclear lysis, and disorganized intermediate filaments

(Figure 3c). The plasma membranes were often damaged leading to the dissociation of desmosomes from the keratin filament network (Figure 3f, arrowheads). Consequently, no RNAs could be isolated from epidermal sheets separated with EDTA (data not shown). Thus, we conclude that the separation of the epidermal sheets by EDTA leads to a loss of cell viability and thereby viral gene expression (Figure 4a).

Ex vivo infection of hair follicles

In addition to the interfollicular epidermis (IFE), we addressed the susceptibility of hair follicles to *ex vivo* infection with HSV-1. Hair follicles represent epidermal appendages that extend into the dermis. The very gentle separation of epidermal sheets from the dermis after dispase II treatment preserved most of the hair follicles and, thus, allowed infection studies. We prepared the epidermis from tail skin during the first telogen phase after morphogenesis at postnatal day (P) 21 to characterize infection during the resting phase of the hair follicles. Upon infection with 10 PFU/cell, many hair germ cells became infected, whereas only a very limited number of infected cells was present in the bulge region that is the niche for the quiescent SCs (Figure 5a). Staining of the sebaceous glands was shown to be unspecific (Rahn *et al.*, 2015). Raising the virus dose to 100 PFU/cell did not increase the number of infected cells in the bulge, suggesting that infection is indeed restricted to the hair germ cells (Figure 5a). In contrast, when we infected the epidermis during anagen at P29, we found that most cells in the bulge were infected, whereas the extended hair germ was again fully infected (Figure 5b). These results suggest that the susceptibility to HSV-1 depends on the cycling phase of the hair follicle.

To further characterize the cell types with high or low HSV-1 susceptibility during telogen, we visualized SCs in the bulge by staining for CD34 and the hair germ cells by staining for P-cadherin. Staining of CD34 did not correlate with ICP0 expression (Figure 5c), suggesting that quiescent CD34-positive SCs do not support infection. In contrast, the cells that expressed ICP0 were also positive for P-cadherin, confirming that these were activated hair germ cells (Figure 5c).

To assess whether proliferating cells in general are preferentially infected, we performed infection studies with the epidermis prepared from BrdU-injected mice. We used a virus dose of 10 PFU/cell, as the 10-fold higher dose led to complete infection of the IFE. When whole mounts were stained at 3 hours p.i., ~ 28% of cells expressed ICP0 in the IFE, whereas ~ 15% of cells were found to be BrdU-positive (Figure 5d). As only a third of the BrdU-positive cells in the IFE expressed ICP0, we conclude that cell division in principle is not a precondition for *ex vivo* infection with HSV-1. In P21 resting hair follicles, BrdU incorporation was restricted to the hair germ and absent in the quiescent bulge SCs, as expected (Figure 5d). Similar to the IFE, ICP0 expression was found in non-dividing as well as in the few dividing germ cells, indicating that proliferation did not correlate with infection (Figure 5d).

To investigate the lack of HSV-1 susceptibility in CD34-positive quiescent bulge SCs, we performed infection studies in epidermal sheets of conditional ILK$^{-/-}$ (ILK-K5) mice. Mice lacking ILK in the epidermis are characterized by epidermal hyperthickening and by impaired development of hair follicles with a progressive growth retardation (Lorenz *et al.*, 2007). At P21, ILK-deficient hair follicles are thick and exhibit an enhanced SC activation, which results in a reduction in CD34-positive cells and an increase in proliferation (Morgner *et al.*, 2015). When ILK-deficient epidermis of P21 mice was infected with HSV-1 at 100 PFU/cell, we found that nearly all cells of the hair follicles were infected, which was clearly distinct from P21 wt follicles (Figure 5e). Immunostaining of ILK-deficient epidermis confirmed the reduced number of CD34-positive cells in the bulge region as compared with the wt bulge (Figure 5c and f). Strikingly, however, many of the CD34-positive cells were infected, which was in contrast to the wt situation (Figure 5c and f). These results suggest that the quiescent CD34-positive SCs in the wt bulge cannot be infected, whereas activated SCs in the ILK-deficient bulge support infection. To exclude the possibility that quiescent CD34-positive cells lack the HSV-1 receptors nectin-1 and HVEM, which direct viral entry into epidermal keratinocytes (Petermann *et al.*, 2015), we performed quantitative reverse transcription-PCR. The results indicate the presence of nectin-1 and HVEM mRNAs in bulge SCs (Figure 5g) and confirm their expression in total keratinocyte preparations (Petermann *et al.*, 2015). In addition, we analyzed surface expression of nectin-1 representing the major HSV-1 receptor in the epidermis (Petermann *et al.*, 2015). Flow cytometric analysis demonstrated the presence of nectin-1 on the surface of CD34-expressing cells, suggesting that bulge SCs are in principle susceptible to HSV-1 (Figure 5h). We hypothesize that activated SCs facilitate HSV-1 access to its receptors in the ILK-deficient bulge, as proliferation *per se* is not a precondition for HSV-1 infection.

DISCUSSION

To advance our knowledge of HSV-1 entry from penetration into individual cells to viral invasion routes into tissue, we established an *ex vivo* infection assay for epidermal sheets, as intact skin samples were found to be resistant to HSV-1 infection. This system allows the analysis of cellular determinants that facilitate or restrict the invasion process of HSV-1 into an intact target tissue. For such a system to be useful, a precondition is the characterization of conditions under which the epidermal cells can be *ex vivo* infected. As intact skin samples could not be efficiently infected, our *ex vivo* infection model concentrates on successful infection of epidermal sheets, which lack the basement membrane. Here, we focused on murine epidermis and demonstrated that all keratinocytes in the basal layer were susceptible to HSV-1 provided that the epidermal sheets were viable and maintain their morphology. If culture conditions or methods of separating the epidermis from the dermis interfered with the integrity of the tissue, the number of infected cells decreased. In epidermal sheets, infection was initiated in basal keratinocytes from where viruses spread to suprabasal layers, indicating that HSV-1 could enter differentiated keratinocytes. This mode of infection might reflect the infection route of reactivated virus, which penetrates the epidermis after leaving

the nerve endings, rather than the route during primary infection. To our knowledge, this is the first report demonstrating the initial steps of HSV-1 infection and their limitations at the cellular level in intact epidermis. On the basis of these results, it will be possible to address the epidermal barriers in detail that interfere with invasion of HSV-1 into tissue via the apical surface of the epidermis in intact skin samples.
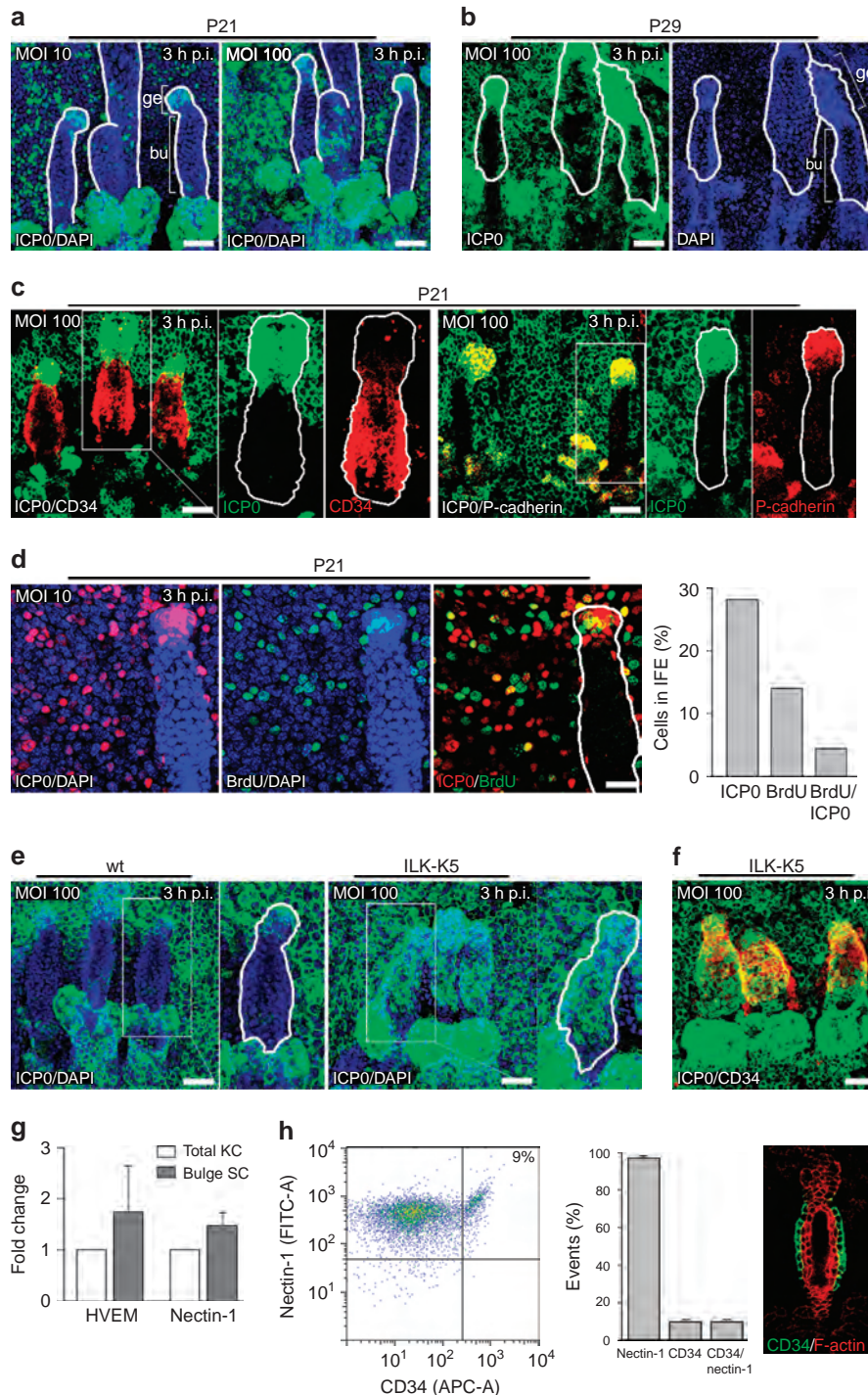

Figure 5. Infection of hair follicles is limited to hair germ at P21. (a and b) Whole mounts of infected epidermis. (c) No CD34-positive cells were infected but P-cadherin-expressing cells. (d) Infected epidermises from BrdU-injected mice demonstrate ICP0 in BrdU- and in not-BrdU-labeled cells. (e) Infected epidermises from wt or ILK-K5 mice (P21) show completely infected ILK-K5 hair follicles and no infection in wt. (f) Infected epidermises of ILK-K5 mice (P21) demonstrate ICP0 in CD34-positive cells. (g) qRT-PCR analysis shows comparable expression of HVEM and nectin-1 in bulge SCs and total keratinocytes (KC) (HVEM: $n = 7$; nectin-1: $n = 8$). (h) Flow cytometry of CD34/nectin-1-positive cells. Results are mean+SD ($n = 3$). One confocal layer of wt hair follicle. Bars, 50 μm (**a**, **b**, **c**, **e** and **f**), 25 μm (**d**). Bu, bulge; Ge, hair germ; HVEM, herpes virus entry mediator; SC, stem cell; wt, wild type.

Although cell proliferation was not a precondition for successful infection of epidermal cells, we observed no infection of quiescent bulge SCs in resting hair follicles, whereas hair germ cells were susceptible. We excluded the possibility that bulge SCs had lost surface expression of nectin-1, which represents the major receptor on epidermal keratinocytes (Petermann *et al.*, 2015). As nectin-1 was present on CD34-positive SCs, we hypothesize that the HSV-1 receptors such as nectin-1 are not accessible as long as the bulge SCs are quiescent. This hypothesis is supported by the observation that ILK-deficient SCs, which are aberrantly activated and fail to establish quiescence, can be efficiently infected (Morgner *et al.*, 2015). We assume that the cell motility of activated SCs facilitates interaction of viral glycoproteins with cell surface structures. Furthermore, attachment of HSV-1 to the cell surface might be modulated in quiescent SCs, leading to reduced entry. Binding to heparan sulfate proteoglycans can enhance HSV entry; yet, their absence does not abolish infection (Spear, 2004). The critical step during transition of the SCs from the quiescent to the activated status might be the re-organization of cell–cell junctions that allows the virus to access its receptors. This supports our observation that infection declines when extended culture periods lead to junctional remodeling. Thus, the intriguing question is how HSV approaches its attachment and fusion receptors in intact tissue and whether a cell's status, by influencing its plasma membrane dynamics, facilitates the receptor accessibility. Our *ex vivo* infection model of epidermal sheets allows very efficient initiation of infection under certain preparation conditions, which remove the basement membrane and maintain the integrity of the basal epidermal layer in culture. How the major receptor nectin-1 and the alternate receptor HVEM are accessible from the basal layer and whether wounding of suprabasal layers is essential for virus access from the apical surface of the epidermis is open for future investigations.

MATERIALS AND METHODS
Mice, preparation of murine epidermis, isolation of primary cells, and viruses
Epidermal sheets were taken from tail skin of adult wt (C57BL/6) or from ILK-K5 mice (Lorenz *et al.*, 2007) as described previously (Petermann *et al.*, 2015; Rahn *et al.*, 2015). Briefly, after incubation of skin samples for 30 minutes at 37 °C with 5 mg ml^{-1} dispase II (Roche, Mannheim, Germany), the epidermis was removed from the dermis as an intact sheet. Alternatively, skin samples were incubated for 4 hours at 37 °C with 5 mM EDTA to remove the epidermis from the dermis. Epidermal sheets were incubated in DMEM/high glucose/GlutaMAX (Life Technologies, Darmstadt, Germany) as described (Rahn *et al.*, 2015). Infection was performed with purified preparations of HSV-1 wt strain 17 (Schelhaas *et al.*, 2003). In brief, virus inoculum was added to the cells at 37 °C, defining time point 0. The calculation of the virus dose was based on the estimated cell number in the basal layer per epidermal sheet (Rahn *et al.*, 2015).

Virus titers were determined by plaque assays on Vero-B4 cells. Infected epidermal sheets were washed at 1 hour p.i., and the titer of cell-released virus was analyzed as indicated.

To maintain murine melanocytes, primary cells were isolated from newborn epidermis as described (Rahn *et al.*, 2015). The cell suspension was cultured on collagen-coated dishes (collagen G; Merck Millipore, Schwalbach, Germany) at 32 °C and maintained in keratinocyte culture medium (DMEM/Ham's F-12 [3.5:1.1]; Merck Millipore) containing 50 μM calcium ions and 10% fetal calf serum (calcium-free), penicillin (400 IU ml^{-1}), streptomycin (50 μg ml^{-1}), adenine (1.8 × 10^4 M), glutamine (300 μg ml^{-1}), hydrocortisone (0.5 μg ml^{-1}), epidermal growth factor (10 ng ml^{-1}), cholera enterotoxin (10^{10} M), insulin (5 μg ml^{-1}), and ascorbic acid (0.05 mg ml^{-1}) in the presence of mitomycin C–treated 3T3 fibroblasts (strain J2). The presence of melanocytes in the primary keratinocytes cultures was visualized by staining against tyrosinase (Hirobe, 1995).

The preparation of epidermal sheets from euthanized mice was in accordance with institutional guidelines on animal welfare and was approved by the North Rhine-Westphalia State Environment Agency, Germany.

Quantitative reverse transcription-PCR
CD34$^+$/α6 integrin^{hi} bulge cells were purified from epidermal cell suspensions by fluorescence-activated cell sorting (FACSAria; BD, Heidelberg, Germany) using CD49f-FITC (BD 555735; 1:500) and eFluor660-conjugated anti-CD34 (eBioscience, Frankfurt, Germany, clone RAM34; 1:100) antibodies. Total RNA was isolated from sorted cells using the RNeasy Plus Mini Kit (Qiagen, Hilden, Germany). cDNAs were synthesized using the High-Capacity cDNA Reverse Transcription Kit (Applied Biosystems, Darmstadt, Germany). qPCR was performed on the StepONE Plus Real-Time PCR System (Applied Biosystems) using the SYBR Green PCR Master Mix (Applied Biosystems) and the following primers: nectin-1 primers (forward, 5′-TGAGGGCTTTGATGGCAACT-3′; and reverse, 5′-AGCCATTCAATGTGGTCCAGT-3′), HVEM primers (forward, 5′-GGAGCCTTTCCAGGAACAAC-3′; and reverse, 5′-ACGTCTCCTCGGTGTCTTGT-3′), and S26 primers (forward, 5′-CGTCTTCGACGCCTACGTGCT-3′ and reverse, 5′-CGGCCTCTTTACATGGGCTTTGGT-3′).

Immuncytochemistry and antibodies
Epidermal whole mounts prepared from murine epidermis (Braun *et al.*, 2003) were fixed with 3.4% formaldehyde, and stained with mouse anti-ICP0 (monoclonal antibody 11060; 1:60) (Everett *et al.*, 1993) followed by incubation with AF488-conjugated anti-mouse immunoglobulin (Ig) G (Life Technologies) and 4′,6-diamidino-2-phenylindole as described (Rahn *et al.*, 2015). In addition, whole mounts were stained with rabbit polyclonal anti-mouse keratin 14 (AF64, Covance, Emeryville, CA; 1:10.000) visualized with AF555-conjugated anti-rabbit IgG (Life Technologies). F-actin was stained with (Atto 565)-conjugated phalloidin (Sigma, Taufkirchen, Germany). Murine epidermal samples were fixed, embedded in Tissue Tek (Sakura, Alphen aan den Rijn, The Netherlands), frozen, cut, and processed as described (Rahn *et al.*, 2015). Briefly, tissue sections were fixed with 0.5% formaldehyde and stained with mouse anti-ICP0 (11060; 1:60) (Everett *et al.*, 1993), the corresponding secondary antibody, and 4′,6-diamidino-2-phenylindole. In addition, cryosections were stained with polyclonal rabbit anti-laminin γ2 (gift from R. Nischt; 1:1500) rat anti-β4 integrin (monoclonal antibody clone 346-11A from SouthernBiotech, Birmingham, AL; 1: 200), or polyclonal rabbit anti-ZO-1 (Life Technologies; 1:400), and the corresponding secondary antibodies.

Primary epidermal cells from wt or Pvrl$^{-/-}$ (nectin-1-deficient) mice (Barron *et al.*, 2008) were fixed with 4% formaldehyde for 15 minutes at room temperature, treated with the Image-iT FX Signal Enhancer (Life Technologies) for 30 minutes, and permeabilized/blocked with 0.01% saponin 10% normal donkey serum (Sigma) for 1 hour. Samples were stained for 60 minutes with anti-ICP0 (monoclonal antibody 11060; 1:60) (Everett *et al.*, 1993) and goat polyclonal anti-mouse tyrosinase (sc-7834, Santa Cruz, Hilden, Germany; 1:50 in 0.01% saponin), followed by staining with the corresponding secondary antibodies and 4',6-diamidino-2-phenylindole for 45 minutes in 0.01% saponin, all at room temperature.

Transmission electron microscopy

Murine epidermal sheets separated from the dermis by either dispase II or EDTA treatment, and epidermal sheets incubated in DMEM for 16 hours at 37 °C after dispase II treatment were prepared for electron microscopy as described (Bechtel *et al.*, 2012). Semithin sections of epidermal sheets were cut, stained with uranyl acetate and lead citrate, and analyzed in a Zeiss 902A electron microscope (Jena, Germany).

Flow cytometric analysis

Murine epidermal sheets were incubated on TrypLE Select (Life Technologies) and processed as described (Petermann *et al.*, 2015). Cell suspensions were incubated in phosphate-buffered saline/5% fetal calf serum on ice for 45 minutes with anti-nectin-1 (CK41; 1:100) (Krummenacher *et al.*, 2000) and eFluor660-conjugated anti-CD34 (eBioscience clone RAM34; 1:100). Nectin-1 was visualized with anti-mouse IgG-AF488 (Life Technologies; 1:200). For nectin-1, mouse IgG1 (Life Technologies) and for CD34 rat IgG2a kappa (eBioschience) were used as isotype controls. Viable cells were assessed by 7-AAD (BD; 1:40) after incubation for 10 minutes on ice. Samples were analyzed by using a FACSCanto II flow cytometer and FACSDiva (version 6.1.3; BD) and FlowJo (version 7.6.3; Tree Star software, Ashland, OR).

REFERENCES

Barron MJ, Brookes SJ, Draper CE *et al.* (2008) The cell adhesion molecule nectin-1 is critical for normal enamel formation in mice. *Hum Mol Genet* 17:3509–20

Bechtel M, Keller MV, Bloch W *et al.* (2012) Different domains in nidogen-1 and nidogen-2 drive basement membrane formation in skin organotypic cocultures. *FASEB J* 26:3637–48

Braun KM, Niemann C, Jensen UB *et al.* (2003) Manipulation of stem cell proliferation and lineage commitment: visualisation of label-retaining cells in wholemounts of mouse epidermis. *Development* 130:5241–55

Boutell C, Everett RD (2013) Regulation of alphaherpesvirus infections by the ICP0 family of proteins. *J Gen Virol* 94:465–81

Bussmann C, Peng W-M, Bieber T *et al.* (2008) Molecular pathogenesis and clinical implications of eczema herpeticum. *Expert Rev Mol Med* 10:e21

Everett RD, Cross A, Orr A (1993) A truncated form of herpes simplex virus type 1 immediate-early protein Vmw110 is expressed in a cell type dependent manner. *Virology* 197:751–6

Foley FD, Greenwald KA, Nash G *et al.* (1970) Herpesvirus infection in burned patients. *N Engl J Med* 282:652–6

Geraghty RJ, Krummenacher C, Cohen GH *et al.* (1998) Entry of alphaherpesviruses mediated by poliovirus receptor-related protein 1 and poliovirus receptor. *Science* 280:1618–20

Gipson IK, Grill SM (1982) A technique for obtaining sheets of intact rabbit corneal epithelium. *Invest Ophthalmol Vis Sci* 23:269–73

Hirobe T (1995) Structure and function of melanocytes: microscopic morphology and cell biology of mouse melanocytes in the epidermis and hair follicle. *Histol Histopathol* 10:223–37

Krummenacher C, Baribaud I, Ponce de Leon M *et al.* (2000) Localization of a binding site for herpes simplex virus glycoprotein D on herpesvirus entry mediator C by using antireceptor monoclonal antibodies. *J Virol* 74:10863–72

Lin JY, Fisher DE (2007) Melanocyte biology and skin pigmentation. *Nature* 445:843–50

Montgomery RI, Warner MS, Lum BJ *et al.* (1996) Herpes simplex virus-1 entry into cells mediated by a novel member of the TNF/NGF receptor family. *Cell* 87:427–36

Morgner J, Ghatak S, Jakobi T *et al.* (2015) Integrin-linked kinase regulates the niche of quiescent epidermal stem cells. *Nat Commun*. in press

Lorenz K, Grashoff C, Torka R (2007) Integrin-linked kinase is required for epidermal and hair follicle morphogenesis. *J Cell Biol* 177:501–13

O'Donnell CD, Kovacs M, Akhtar J *et al.* (2010) Expanding the role of 3-O sulfated heparan sulfate in herpes simplex virus type-1 entry. *Virology* 397:389–98

Petermann P, Haase I, Knebel-Mörsdorf D (2009) Impact of Rac1 and Cdc42 signaling during early herpes simplex virus type 1 infection of keratinocytes. *J Virol* 83:9759–72

Petermann P, Thier K, Rahn E *et al.* (2015) Entry mechanisms of Herpes Simplex Virus Type 1 into murine epidermis: Involvement of nectin-1 and HVEM as cellular receptors. *J Virol* 89:262–74

Rahn E, Thier K, Petermann P *et al.* (2015) Ex vivo infection of murine epidermis with herpes simplex virus type 1. *J Vis Exp* (in press)

Schelhaas M, Jansen M, Haase I *et al.* (2003) Herpes simplex virus type 1 exhibits a tropism for basal entry in polarized epithelial cells. *J Gen Virol* 84:2473–84

Shenoy R, Mostow E, Cain G (2015) Eczema herpeticum in a wrestler. *Clin J Sport Med* 25:e18–9

Shieh MT, WuDunn D, Montgomery RI *et al.* (1992) Cell surface receptors for herpes simplex virus are heparan sulfate proteoglycans. *J Cell Biol* 116:1273–81

Shukla D, Liu J, Blaiklock P *et al.* (1999) A novel role for 3-O-sulfated heparan sulfate in herpes simplex virus 1 entry. *Cell* 99:13–22

Spear PG (2004) Herpes simplex virus: receptors and ligands for cell entry. *Cell Microbiol* 6:401–10

Sprecher E, Becker Y (1986) Skin Langerhans cells play an essential role in the defense against HSV-1 infection. *Arch Virol* 91:341–9

Taylor JM, Lin E, Susmarski N *et al.* (2007) Alternative entry receptors for herpes simplex virus and their roles in disease. *Cell Host Microbe* 2:19–28

Wollenberg A, Wetzel S, Burgdorf WH *et al.* (2003) Viral infections in atopic dermatitis: pathogenic aspects and clinical management. *J Allergy Clin Immunol* 112:667–74

Yoon M, Zago A, Shukla D *et al.* (2003) Mutations in the N termini of herpes simplex virus type 1 and 2 gDs alter functional interactions with the entry/fusion receptors HVEM, nectin-2, and 3-O-sulfated heparan sulfate but not with nectin-1. *J Virol* 77:9221–31